



Article

Temporal Changes in Land Use, Vegetation, and Productivity in Southwest China

Xuan Li 10, Li Rong 1,*, Mengmeng Zhang 1, Wensong Yang 1, Zhen Zeng 1, Chengjun Yuan 2 and Qi Wang 1,2

- School of Geography and Environmental Sciences, Guizhou Normal University, Guiyang 550000, China
- ² School of Karst Science, Guizhou Normal University, Guiyang 550001, China
- * Correspondence: ronglit@gznu.edu.cn

Abstract: In recent decades, vegetation coverage and land use/land cover (LULC) have constantly changed, especially in southwest China. Therefore, it is necessary to conduct in-depth research into the temporal–spatial variation patterns of vegetation greening, LULC, and gross primary productivity (GPP). Here, we used remote sensing to analyze the spatial and temporal variation in the normalized difference vegetation index (NDVI) and GPP in the growing season under different LULCs in southwest China. Results showed: (1) From 2000–2019, the forest area in southwest China had increased by 2.1%, while the area of cropland and grassland had decreased by 3.2% and 5.5%, respectively. Furthermore, there are significant differences in spatial variation patterns. (2) NDVI and GPP in the growing season showed a general increasing trend (p < 0.01); vegetation coverage is dominated by high coverage to highest coverage and medium coverage to high coverage transfer. (3) Under different LULCs, the migration directions of NDVI and GPP were different. The center of gravity migration of highest and medium coverage shifted to the southeast by 1.69° and to the northwest by 1.81°, respectively. The results showed the ecosystem evolution and will help to guide the maintenance measure of ecosystem balance and sustainable development.

Keywords: southwest China; normalized difference vegetation index (NDVI); gross primary productivity (GPP); land use/land cover (LULC); center of gravity shift model



Citation: Li, X.; Rong, L.; Zhang, M.; Yang, W.; Zeng, Z.; Yuan, C.; Wang, Q. Temporal Changes in Land Use, Vegetation, and Productivity in Southwest China. *Land* **2022**, *11*, 1331. https://doi.org/10.3390/land11081331

Academic Editor: Xiaoyong Bai

Received: 19 July 2022 Accepted: 15 August 2022 Published: 17 August 2022

Publisher's Note: MDPI stays neutral with regard to jurisdictional claims in published maps and institutional affiliations.



Copyright: © 2022 by the authors. Licensee MDPI, Basel, Switzerland. This article is an open access article distributed under the terms and conditions of the Creative Commons Attribution (CC BY) license (https://creativecommons.org/licenses/by/4.0/).

1. Introduction

The ecological environment of karst landforms in southwest China is fragile and has been significantly affected by climate and human activities in recent decades [1–3]. Changes in vegetation, LULC, and GPP affect biogeochemical cycles, and social effects in this region impact the area range of influence [4–7]. However, the spatial and temporal characteristics of LULC, vegetation, and carbon storage are not clear. This has a significant impact on ecological evolution and regional social development [8,9]. Therefore, there is a need to clarify the temporal change characteristics of LULC, vegetation, and carbon storage in southwest China.

Southwest China has a large number of karst ecosystems, which are hypersensitive and fragile. First, this area is one of the largest exposed areas of carbonate rock salts in the world [10], and in these environments, the soil formation rate is low, and the permeability is high due to the presence of interstitial fractures. Furthermore, it has unique and fragile geomorphological and hydrogeological features [11]. In recent decades, long-term and severe climate change and human activities have brought enormous pressure to the ecosystem in this area [12–14]. Rocky desertification has become one of the most serious environmental problems in karst areas [15,16]. Terrestrial vegetation types and compositions have changed due to climatic conditions, carbon dioxide fertilization effects, and LULC [17,18]. Second, under the background of population pressure and urbanization, the intensity of human activities has increased rapidly, and the land cover has undergone drastic changes [19]. Third, since the end of the 20th century, China has implemented a large number of ecological

Land 2022, 11, 1331 2 of 18

engineering constructions, which have achieved an increase in vegetation coverage and carbon storage through ecological restoration and improved ecosystem services [20–22]. In addition, the southwest region is an important ecological barrier and ecologically fragile, with extensive potential for various ecosystem services, such as soil and water conservation, climate regulation, and carbon balance [23–25], providing a huge contribution to social development, ecosystem balance and carbon sequestration [24,26,27].

At present, the spatial and temporal changes in LULC, vegetation cover, and gross primary productivity (GPP) in southwest China are not clear. Vegetation is an important factor affecting the ecological balance and is usually considered as a direct and obvious indicator to analyze the impact of natural seasonal changes and human activities on the ecological environment [28,29]. Gross primary productivity (GPP) is an important indicator reflecting vegetation status, ecosystem structure, and function [30] and plays a key role in carbon cycling in terrestrial ecosystems [31], and is an important factor in measuring the regional ecological value [32,33]. Therefore, clarifying temporal and spatial evolution processes is of great significance for understanding the value and sustainable development of ecosystems. Studies have found that China's vegetation has shown an overall greening trend in the past 30 years [24]. However, due to the vast heterogeneity of climate, topography, and human activities in the southwest, the spatial and temporal distributions of LULC, vegetation dynamics, and gross primary productivity (GPP) are significantly different [2,14,34]. Since 2000, the LULC change in southwest China has been mainly manifested in the expansion of forest land and the reduction in cropland [4,35]. The study found that NDVI increased significantly in low- to mid-altitude areas < 3400 m due to improved afforestation and agricultural productivity [36]. In the afforestation and grassland restoration areas, the direct contribution of forest land to the annual growth rate of GPP is 24.64% [37]. In addition, according to long-term remote sensing vegetation data, it is found that short-term extreme climate events respond differently to different land-use types, resulting in differences in regional ecological effects [38,39]. Therefore, it is of great significance to understand the temporal and spatial pattern characteristics and change processes of different LULC types, vegetation dynamics, and gross primary productivity in the region for correctly understanding the temporal dynamic changes and spatial changes in regional vegetation dynamics and gross primary productivity.

The changes in vegetation and productivity center can reflect the evolution of ecosystems influenced by human activities and climate change. Human activities affect vegetation and productivity changes, such as ecological engineering, which increases vegetation growth and carbon storage in southwest China [40,41], and positively contributes to vegetation productivity [42]. However, the expansion of arable land and the surge in population has also led to the degradation of vegetation [15]. Deforestation reduced the GPP and leaf area index in China between 1982 and 2011, and their centers of gravity shifted [43]. The spatial and temporal changes in vegetation cover and productivity in different regions have obvious uncertainties [6,44,45]. Natural evolution is also an important factor leading to the migration of its center of gravity; for example, the northward shift of the climatic zone makes the ecological center of gravity move northward [46,47]. In summary, combined with different LULC types, studying the temporal and spatial variation patterns of different levels of vegetation cover (NDVI) and its gross primary productivity (GPP) in southwest China can deepen the understanding of vegetation and productivity changes in southwest China. It has very important ecological value and practical significance for the balance and sustainable development of the ecosystem.

The purpose of this study is to clarify the temporal and spatial dynamic of LULC, vegetation cover, and GPP in southwest China and the migration pattern of the center of gravity. Combined with MODIS remote sensing, we analyzed the temporal and spatial changes of vegetation cover (NDVI) and gross primary productivity (GPP) under different LULC types in southwest China. Therefore, our aims in the study are: (1) to clarify the migratory direction of LULC in southwest China and the spatial and temporal change patterns of NDVI and GPP in the growing season; (2) to explore the change characteristics of

Land 2022, 11, 1331 3 of 18

GPP under different land use types and different vegetation coverage levels; (3) to analyze the migration law of vegetation cover and GPP center of gravity.

2. Data and Methods

2.1. Study Area

Southwest China covers a region bounded by $20^{\circ}54'-34^{\circ}19'$ N and $97^{\circ}21'-112^{\circ}04'$ E (Figure 1). It includes five provinces (municipalities, autonomous regions): Chongqing, Sichuan, Guizhou, Yunnan, and Guangxi. The area has a total coverage of 1.38×106 km², which is about 14.34% of China. The study area is dominated by the subtropical monsoon climate, affected by the southeast and the southwest monsoon, with a mean annual temperature of 14.6 °C and an average annual precipitation of 1195 mm, of which 600 mm occurs in the growing season. The terrain is high in the west and low in the east, with a stepped distribution, diverse landform types, and high landscape heterogeneity [48]. Southwest China is the most concentrated area of karst landforms, accounting for 23.14% of China's karst distribution area. The forest has a large area and is widely distributed in the study area. Grassland is mainly distributed in the western Sichuan Plateau, and cropland is mainly distributed in the Sichuan Basin, the middle of the Guangxi hills, and the eastern part of the Yunnan–Guizhou Plateau. The three main LULC types are grassland, forest, and cropland, accounting for more than 98% of the total area of southwest China.

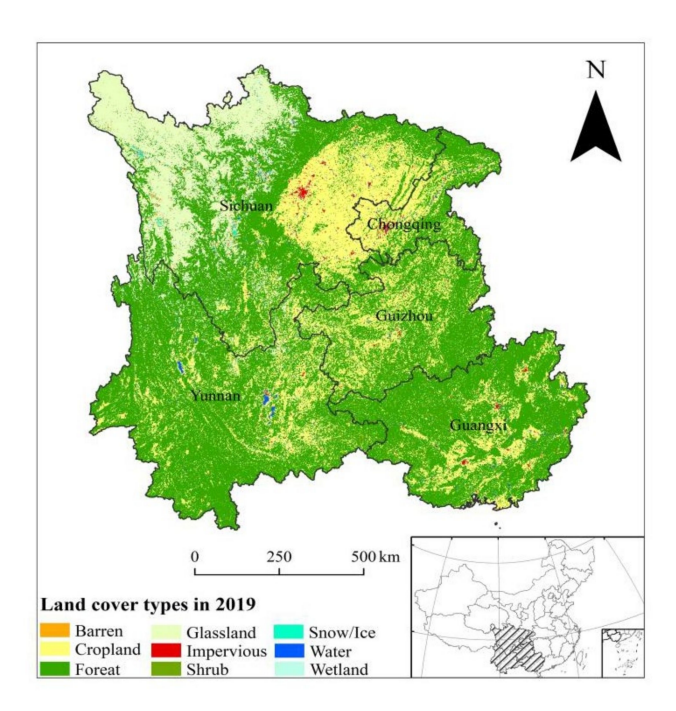


Figure 1. Study area location in China and land cover types in 2019.

2.2. Data

The normalized difference vegetation index (NDVI) data came from the study derived from the MOD13A2 data product, with a spatial resolution of 1 km and a temporal resolution of 16d (https://ladsweb.modaps.eosdis.nasa.gov/ (accessed on 6 August 2021)). These data were preprocessed on the Google Earth engine platform (https://earthengine.google.com (accessed on 6 August 2021)), and the NDVI data from May to September 2000–2019 were downloaded. The gross primary productivity (GPP) datasets were obtained from the MOD17A2HV6 data product with a spatial resolution of 500 m and a temporal resolution of 8d (https://lpdaac.usgs.gov/products/mod17a2hv006/ (accessed on 28 August 2021)), and we downloaded the contemporaneous datasets from the Google Earth engine platform (https://earthengine.google.com (accessed on 28 August 2021)). The LULC data came from the first Landsat-derived annual China Land Cover Dataset

Land 2022, 11, 1331 4 of 18

(CLCD) from 1990 to 2019, with a spatial resolution of 30 m and an overall accuracy rate of 79.31%, better than MCD12Q1, ESACCI_LC, FROM_GLC, and GlobaLand30. The LULC types in these data were divided into nine categories: cropland, forest, shrub, grassland, water, snow/ice, barren, impervious, and wetland. The CLCD dataset introduced in this article is freely available at http://doi.org/10.5281/zenodo.4417810 (accessed on 10 August 2021) [49].

2.3. Methods

The normalized difference vegetation index (NDVI) can reflect the growth and coverage of surface vegetation [50,51]. Therefore, the NDVI values of different LULC types were extracted to represent the growth state of this vegetation type. Vegetation has obvious inter-annual and seasonal variation characteristics, and its NDVI value in the season of the most active growth stage can more accurately represent the vegetation growth state in this region [52]. In order to reduce the NDVI error caused by the seasonal changes in vegetation, this paper used NDVI and GPP values in the growing season (May–October) to analyze vegetation activities, which accurately reflected the status of vegetation cover and GPP in southwest China. To minimize the effect of cloud contamination and atmospheric variability, we calculated the annual growing season NDVI by using the maximum value composites (MVC) method [53]. The MODIS NDVI and GPP data in the study area were resampled to the monthly scale using ArcGIS10.4, with a spatial resolution of 1 km. Additionally, by averaging each pixel, the average values from May to October were obtained as the growing season NDVI and GPP for each year from 2000 to 2019, which meant in pixels of 500×500 , there was, on average, one gC unit of GPP per 1 m².

Simple linear regression was used to analyze the annual trends of average NDVI and GPP values in the growing season of different LULC in southwest China from 2000–2019. All data were analyzed using Python software. Additionally, referring to related research [54], the vegetation coverage was divided into lowest coverage ($0 < \text{NDVI} \le 0.35$), low coverage ($0.35 < \text{NDVI} \le 0.55$), medium coverage ($0.55 < \text{NDVI} \le 0.75$), high coverage ($0.75 < \text{NDVI} \le 0.85$), and highest coverage ($0.85 < \text{NDVI} \le 1$), five grades. The gravity center migration can show the change directions in the region's center of gravity. Therefore, the change directions in the region's NDVI and GPP gravity centers were calculated by gravity center migration. This, in turn, can reflect the import of human activities or climate change on the migration of vegetation zone. The main LULC types in southwest China were cropland, forest, and grassland, and other land types (shrub, water, snow/ice, barren, impervious, and wetland) accounted for only 2% of the total area (Figure 1). Therefore, this paper mainly analyzed the change characteristics of three LULC types of cropland, forest, and grassland, the temporal and spatial distribution of NDVI and GPP in the growing season of different LULC types, as well as the regular change in the center of gravity.

3. Results

3.1. Land Types Changes

During the study period, the composition of LULC types in the study area changed significantly, with a high spatial heterogeneity between the LULC types (Figure 1). The conversion of farmland into forests was the major driving force of LULC change. Overall, the forest area showed increasing trends after 2000, but it showed a decreasing trend first and then increased ($1.04\,\mathrm{year}^{-1}$, p < 0.01). Forest area increased by $16,180.0\,\mathrm{km}^2$, accounting for 58.7% of the regional area from 2000 to 2019 (Figure 2, Table 1). The growing regions of forest were mainly distributed in northeastern Sichuan and southwestern Yunnan, and the decreasing regions were mainly distributed in southeastern Guizhou, northwestern Guangxi, and northwestern Yunnan. The cropland area first increased and then decreased, showing a significant downward trend overall ($-0.707\,\mathrm{year}^{-1}$, p < 0.01). The area of conversion of farmland into forests was $61,318.48\,\mathrm{km}^2$, which was the LULC change type with the greatest land area transfer, mainly concentrated in the Sichuan Basin, northern Guizhou, and central and southern Guangxi (Figure 1). The grassland area showed a

Land 2022, 11, 1331 5 of 18

continuously decreasing trend (-0.64 year⁻¹, p < 0.01), of which 10,948.30 km² of the grassland area was converted into forest. The change regions were concentrated in the Hengduan Mountains in the northwest of Yunnan, Kunming–Zhaotong regions in the northwest, and the western Sichuan plateau region. A grassland area of 4231.28 km² was converted into cropland, the change regions were mainly concentrated in the northeast part of Yunnan, the western part of Guizhou, and there were also sporadic changes in southern Sichuan.

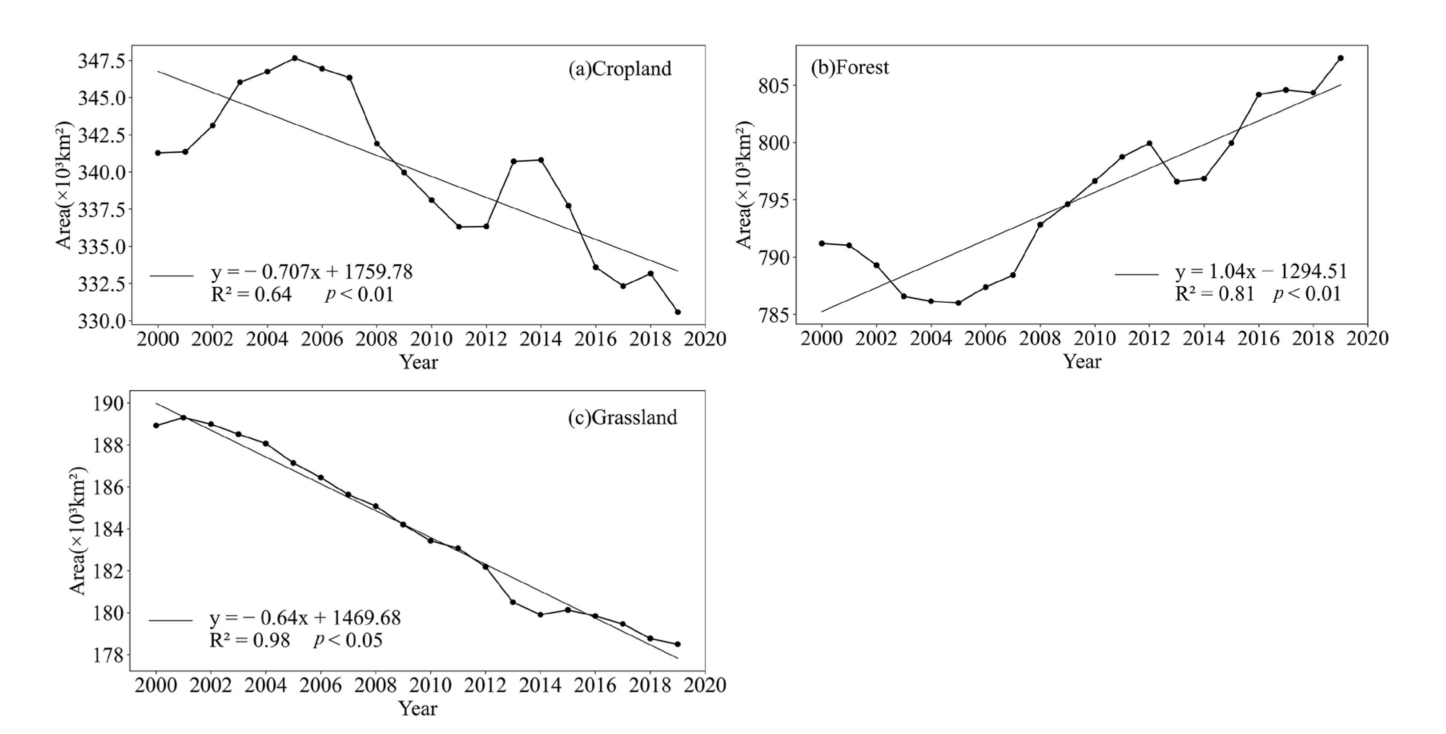


Figure 2. Changes in area of different LULC types: (a) cropland, (b) forest, (c) grassland. (Note: the black solid line represents the trend line, and the formula of cropland is y = -0.707x + 1759.78; the formula of forest is y = 1.04x - 1294.51; the formula of grassland is y = -0.64x + 1469.68).

Table 1. Transformation matrix of land cover types from 2000 to 2019 (km²).

2000–2019	Cropland	Forest	Grassland
Cropland	264,799.33	61,318.48	3956.10
Forest	55,715.85	719,978.95	4073.26
Grassland	4231.28	10,948.30	166,551.06

3.2. The Characteristics of Inter-Annual Variation in NDVI

From 2000 to 2019, the average NDVI of vegetation in the growing season in the whole study area showed an overall upward trend with fluctuations (slope = 0.0023 year^{-1} , p < 0.01). The growing season average NDVI values of different land cover types all showed an increasing trend, but there were some differences. Among them, forest had the highest NDVI value, ranging from 0.79 to 0.84; cropland NDVI value ranged from 0.74 to 0.79; grassland vegetation NDVI varied from 0.70 to 0.73 (Figure 3b). The increase in the NDVI of forest was 0.0025 year⁻¹, and the trend of NDVI of cropland was 0.0023 year⁻¹, which was twice the increase in grassland (0.0011 year⁻¹).

Land 2022, 11, 1331 6 of 18

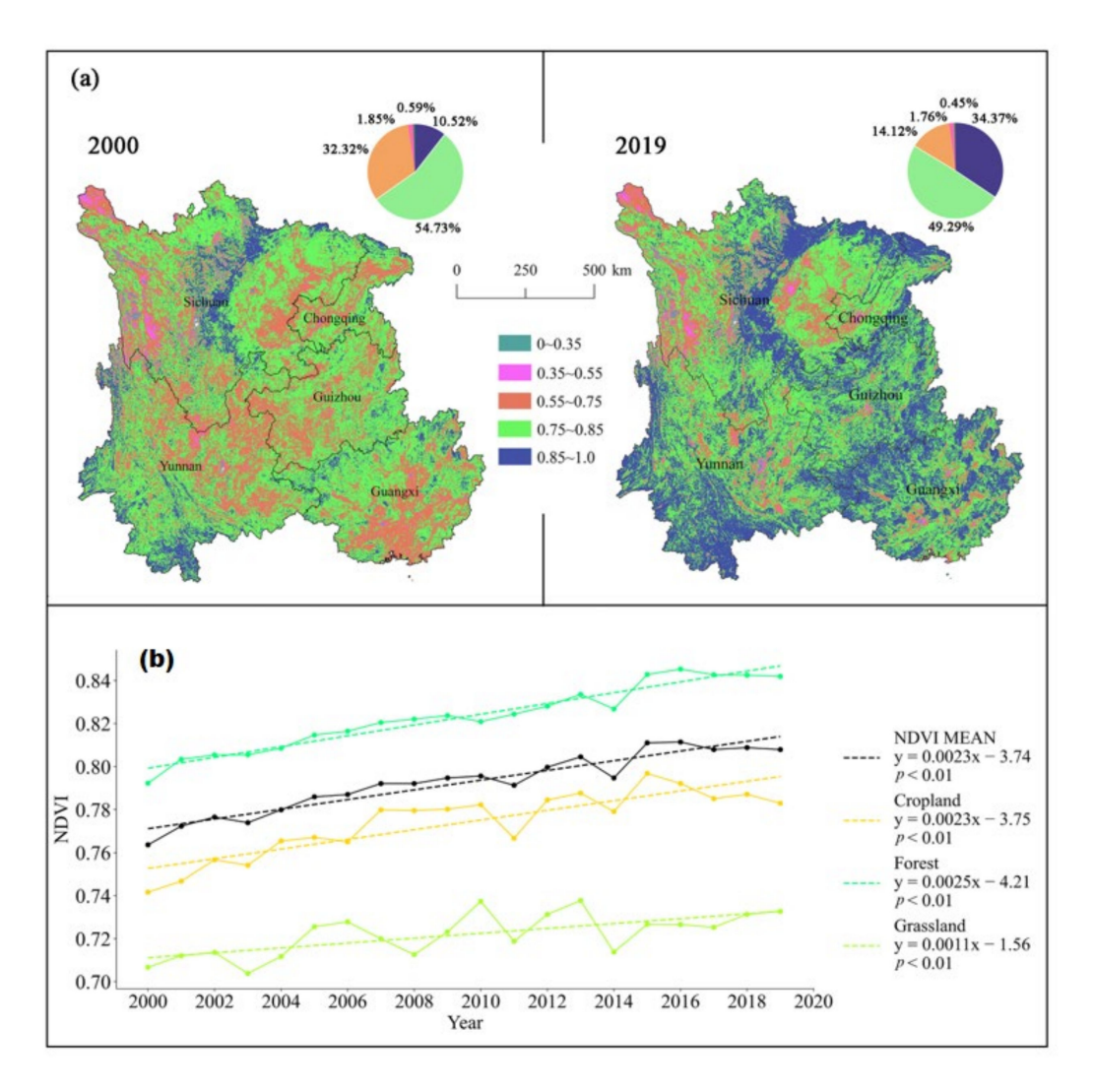


Figure 3. (a) Spatial distribution of NDVI in southwest China and (b) Changing trends in NDVI values from 2000 to 2019 for different land use types.

The vegetation coverage in southwest China in 2000 was dominated by medium and high coverage, accounting for 87.05% of the regional area. In 2019, the vegetation coverage was dominated by highest and high coverage, accounting for 83.66% of the regional area. In terms of spatial distribution, there was a large heterogeneity in the level of surface cover (Figure 3a). The coverage situation in the southwest region showed that the area of lowest coverage, low coverage, medium coverage, and high coverage decreased, but the area of highest coverage increased. Overall, the degree of the greening of vegetation was strengthened. From 2000 to 2019, the area of highest coverage (0.85~1.0) increased from 10.52% to 34.37%, and the main change region was concentrated on the edge of the Sichuan Basin and the three provinces of Yunnan, Guizhou, and Guangxi, with the land cover being forest. The area of high coverage (0.75~0.85) decreased from 54.73% to 49.30%, mainly concentrated in the Sichuan Basin, the eastern Yunnan-Guizhou Plateau, and the northern hills of Guangxi, with the land cover being mainly cropland and forest. The area of medium coverage (0.55~0.75) decreased the most from 32.32% to 14.12%. The main change region was distributed in the Yunnan-Guizhou Plateau, with the cover area being mainly grassland and cropland. There was little change in the low coverage (0.35~0.55) and lowest coverage (0~0.35), which decreased from 2.70% to 2.21%, with the main type of cover being grassland, distributed in the northwest of Sichuan. The vegetation cover types remained unchanged at 48.66% of the total area, while vegetation cover improved to 45.60%.

Land 2022, 11, 1331 7 of 18

From 2000 to 2019, the vegetation cover in southwest China mainly shifted from "high coverage to highest coverage" and "medium coverage to high coverage and highest coverage" (Table A1). The specific transfer amount was as follows: the area from high coverage to highest coverage was 311,870.61 km², accounting for 44.17% of the total change, and the area from medium coverage to high coverage was 259,673.48 km², accounting for 36.77% of the total change. From the perspective of the final change, the transfer-out area of high coverage was the largest, which was 357,704.37 km², 1.26 times the transfer-in area, accounting for 50.66% of the total transfer-out area; the highest coverage transfer-out area was 23,192.33 km², accounting for 3.28% of the total transfer-out area; the medium coverage transfer-out area was 307,709.17 km², accounting for 43.58% of the total transfer-out area and 5.36 times the transfer-in area; the low coverage transfer-out area was 13,993.99 km², accounting for 1.98% of the total transfer-out area; and the transfer-out area of lowest coverage was 3544.33 km², accounting for 0.5% of the total transfer-out area. The transferin area of highest coverage was the largest, which was 351,279.44 km², accounting for 49.75% of the total transfer-in area, and 15.15 times the transfer-in area; the high coverage transfer-in area was 283,127.25 km², accounting for 40.10% of the total transfer-in area; the area of medium coverage transfer-in area was 57,361 km², accounting for 8.12% of the total transfer-in area; the transfer-in area of low coverage was 12,805.25 km², accounting for 1.81% of the total transfer-in area; and the transfer-in area of lowest coverage was 1570.49 km², accounting for the total transfer-in area of 0.22%. In this period, the vegetation coverage mainly showed a trend of gradual improvement, and the vegetation coverage also gradually increased.

3.3. GPP Changes

Since 2000, the overall trend of the annual mean value of GPP in the growing season in the study area increased significantly, with a change rate of 3.65 gC·m⁻²year⁻¹ (p < 0.01). From 2000 to 2019, the average GPP in the growing season increased from 553.77 gC·m⁻² to 624.33 gC·m⁻², an increase of 12.74% (Figure 4a). Among them, the average value of GPP in the growing season was the lowest at 553.77 gC·m⁻² in 2000, and the average value was the highest at 728.83 gC·m⁻² in 2016. During the study period, the GPP of the three land cover types showed an increasing trend. Cropland and forest showed a significant increasing trend (p < 0.01), while grassland showed a slight upward trend (p > 0.05). The GPP of different land cover types showed a great difference in growing seasons, and the GPP of forest and cropland had a high coincidence with the overall GPP trend in southwest China. Forest was the land cover type with the highest gross primary productivity, and the highest average GPP in the growing season was 654.7 gC·m⁻²; the second was cropland, which was 571.63 gC·m⁻²; and the lowest value of grassland was 420 gC·m⁻². Since forest had the highest average GPP, the transfer of forest to other land cover types led to a decrease in GPP, and the conversion of cropland and grassland to forest led to an increase in GPP. In general, the carbon storage of land cover increased, indicating that the ecological environment in southwest China improved.

The average value of the growing season in southwest China from 2000 to 2019 was 594.61 gC·m⁻², which showed a decreasing trend from southeast to northwest, corresponding to the distribution of cropland, forest, and grassland, with significant spatial differences. The high-value regions of GPP were mainly distributed in northwestern Yunnan, southeastern Guangxi, Sichuan Basin, etc. In addition, the GPP was relatively large in central and southern Guizhou, which was covered by forest and cropland. However, the concentrated distribution region of grassland in northwestern Sichuan, the concentrated distribution region of cropland in the Sichuan Basin, and the GPP value were generally lower than the average value (Figure 4b).

Land 2022, 11, 1331 8 of 18

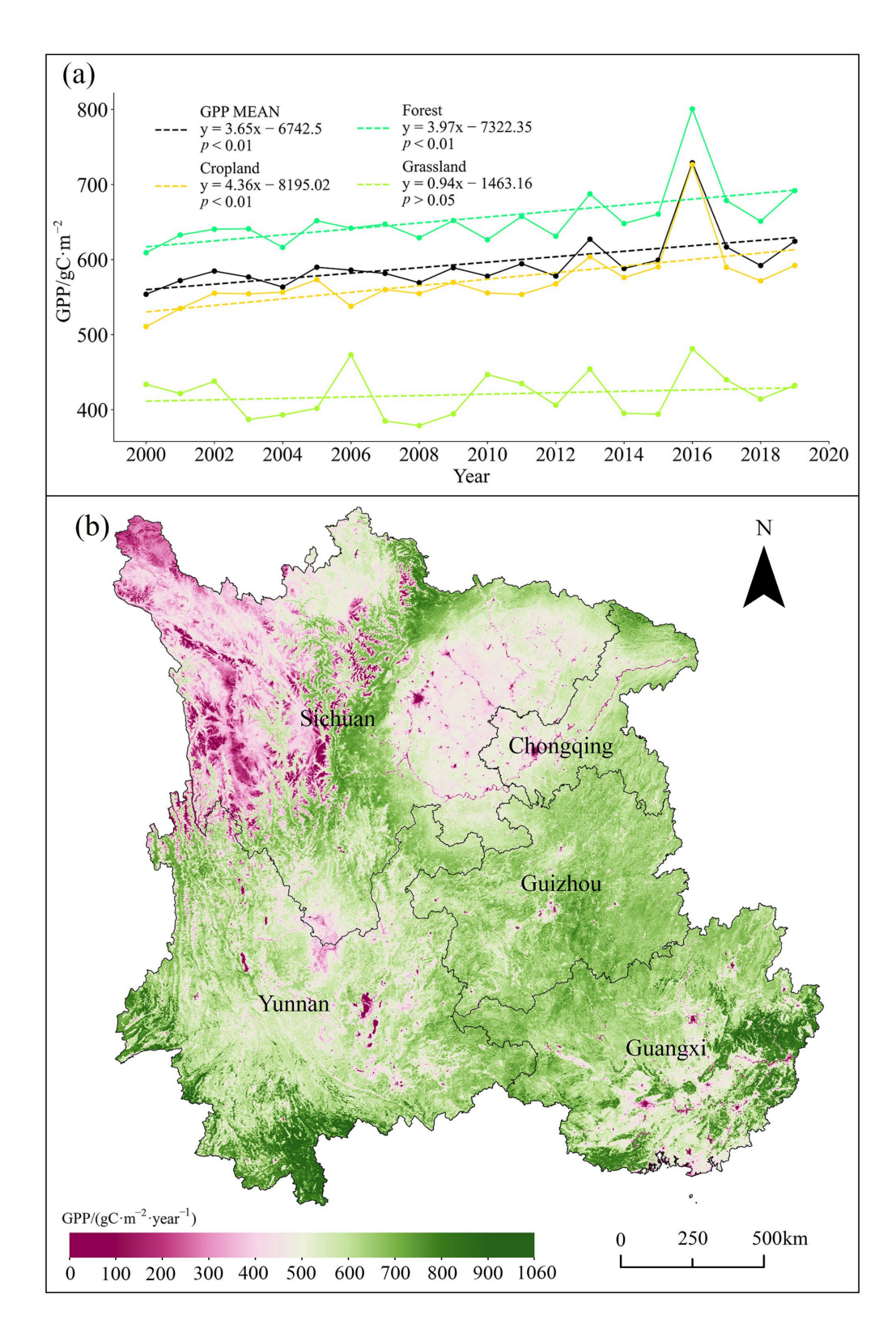


Figure 4. (a) Interannual GPP changes in different land use types; the dashed line shows the variation trend of GPP in different land use types, where the black is GPP mean, the formula is y = 3.65x - 6742.5; the yellow is cropland's GPP, the formula is y = 4.36x - 8195.02; the cyan is forest's GPP, the formula is y = 3.97x - 7322.35; the light green is grassland's GPP, the formula is y = 0.94x - 1463.16 and (b) spatial distribution pattern of GPP values of different land cover types in Southwest China from 2000 to 2019.

Land 2022, 11, 1331 9 of 18

3.4. Changes in the Center of Gravity of NDVI and GPP

From 2000 to 2019, the migration direction of the NDVI center of gravity of different land cover types also showed varying differences. The center of gravity of the NDVI value of cropland moved to the southwest by 0.12° in the meridian and 0.12° in latitude. Among them, the center of gravity of cropland moved in the southeast direction, moving 0.037° in the meridian and 0.12° in latitude from 2000 to 2005; the center of gravity moved in the west direction, moving 0.16° in the meridian and 0.01° in latitude from 2005 to 2019; and the center of gravity of the woodland moved to the northeast, moving 0.03° in the meridian and 0.06° in latitude. However, the center of gravity moved to the northwest from 2000 to 2005 and continued to move to the northwest from 2000 to 2019 by 0.06° in the meridian and 0.16° in latitude. Since 2000–2006 was the main implementation period of the ecological project, the composition of land cover changed greatly, and the change direction of the NDVI center of forest, cropland, and grassland changed (Figure 5).

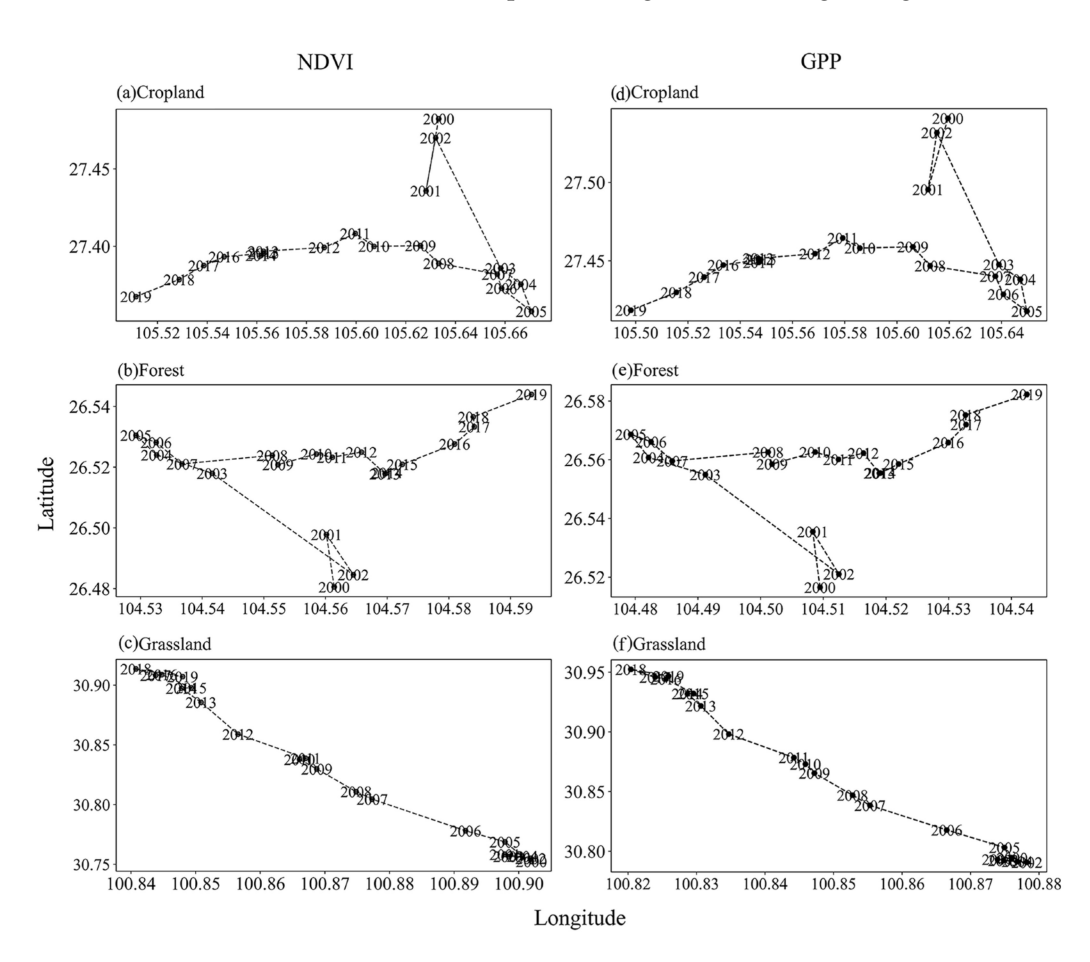


Figure 5. Changes in the center of gravity of NDVI and GPP. (Note: (a–c): Changes in the NDVI center of gravity of cropland, forest and grassland from 2000 to 2019; (d–f) Change in the GPP center of gravity of cropland, forest and grassland from 2000 to 2019).

The study found that the migration direction of the GPP gravity center of the same type of LULC type had been consistent with the gravity center migration direction of its NDVI (Figure 5). During the study period, the center of GPP of cropland moved to the southwest. The GPP center of gravity of cropland moved to the southeast from 2000 to 2005, by 0.03° in the meridian and 0.12° in latitude, while the GPP center of gravity of cropland moved to the southwest from 2005 to 2019, and the migration amplitude increased, moving 0.15° in the meridian, while there was almost no change in latitude. The GPP center of gravity of the forest moved to the northeast. From 2000 to 2005, it first moved to the

Land 2022. 11, 1331 10 of 18

northwest, moving 0.03° in the meridian and 0.052° in latitude, and then it moved to the northeast, moving 0.063° in the meridian and 0.014° in latitude. The GPP center of gravity of the grassland continued to move to the northwest in the study period, by 0.05° in the meridian and 0.15° in latitude.

From 2000 to 2019, the center of gravity of the lowest coverage shifted to the southeast, moving 0.36° in the meridian direction and 0.24° in the latitudinal direction, with a small but complex change in the inter-annual migration direction. The center of gravity of low coverage also moved to the southeast, 0.77° in the longitudinal and 0.24° in the latitudinal direction. During 2000–2008, the low coverage center of gravity first shifted back and forth to the northwest, and then folded to the southeast after 2008. The medium coverage center of gravity moved to the northwest, with a larger migration range, moving 1.24° in the meridian and 1.14° in the latitudinal direction. The center of gravity of the high coverage migrated to the northwest but migrated to the southeast first from 2000 to 2011, moving 0.157° in the meridian and 0.01° in latitude. After 2011, it migrated to the northwest, moving 0.26° in the meridian and 0.08° in latitude; the center of gravity of the highest coverage migrated to the southeast as a whole, moving 1.32° in the meridian and 0.53° in latitude (Figure A1).

Under different vegetation coverage levels, the migration direction of the gravity center of GPP was basically the same as that of vegetation NDVI (Figure A1). During the study period, the gravity center of GPP of lowest coverage and low coverage migrated to the southeast direction, with 0.36° and 0.77° in longitude, respectively, with a latitude migration of 0.24° for both. The center of gravity of the GPP with medium coverage moved to the northwest, moving 1.30° in the meridian and 1.19° in latitude. The center of gravity of the high-coverage GPP moved to the southeast from 2000 to 2008, moving 0.21° in the meridian and 0.22° in the latitudinal direction, then turned around and moved to the northwest direction after 2008, moving 0.31° in the meridian direction, and 0.30° in the latitudinal direction. The center of gravity of the highest-coverage GPP moved to the southeast direction, moving 1.37° in the meridian direction and 0.61° in the latitudinal direction.

4. Discussion

4.1. Spatiotemporal Variation in Land Types and NDVI and GPP

The results revealed that the rate of returning farmland to forest increased significantly in the study period (2000–2019), and cropland was the main land source for forest expansion. The area changes of LULC types were as follows: the area of cropland increased first and then decreased, while the area of forest decreased first and then increased, and the grassland continued to decrease in southwest China (Figure 2). This trend was consistent with the trend of land-use change in China [19]. In the study region, cropland was mainly distributed in the east of Sichuan, the center of Guangxi, the west of Guizhou, and the east of Yunnan (Figure 1). These regions were suitable for agricultural activities due to their flat terrain. The increase in agricultural intensification and productivity has led to the expansion of cropland in these regions, the main source of which was forest and grassland. Due to the development of ecological engineering, the phenomenon of "returning farmland to forest" appeared in the margin of Sichuan Basin, northwest and southwest Yunnan, southeast Guizhou, and south Guangxi, which effectively controlled the expansion of cropland. This indicates that the ecological restoration project in this region was the main driver of LULC change in most regions of southwest China and has achieved some results at this stage [55]. Second, rapid urbanization was also one of the most common causes of farmland loss [56]. At the beginning of the 21st century, the urban area of the Sichuan Basin increased by 66,000 hm², accounting for 68.31% of the decreased area of cultivated land [57]. The grassland was mainly concentrated in the northwestern part of Sichuan, where the altitude is higher, combined with a cold and dry climate. There are rivers flowing through this region, and the precipitation is relatively abundant. Under the background of climate warming, this is conducive to the growth of vegetation, and with the LULC change, in some regions, grassland has shifted to forest.

Land 2022, 11, 1331 11 of 18

The study found that the NDVI and GPP of vegetation in the growing season had shown a significant upward trend as a whole, and the growth trends had been different for different LULC types in southwest China from 2000 to 2019 (Figures 3b and 4a). This is consistent with the conclusion that the main vegetation types in China show a dynamic greening trend, which is the result of the combined effects of climate change, LULC types of distribution, and human activities (such as ecological engineering and agricultural management), among other factors [58–60]. In general, the increase in the NDVI value in southwest China was mainly due to ecological restoration caused by ecological projects such as returning farmland to forest, natural forest protection plans, and closing mountains for afforestation [55,61]. The average NDVI and GPP of vegetation in the growing season in southwest China were high in the southeast and low in the northwest (Figures 3a and 4b), which was mainly related to the spatial distribution of LULC types. In southwest Yunnan, southeast Guangxi, and Sichuan Basin, high mean NDVI and GPP levels in the growing season were mainly distributed in forests, while northwest Sichuan and Sichuan Basin were mainly distributed in grasslands and croplands, which were lower than those of forests on the whole. Compared with 2000, most regions became greener and more productive in 2019. The conversion of a large amount of cropland or grassland to forest and the ecological restoration of most regions (low coverage shift to high coverage) resulted in significant greening of vegetation. However, at the periphery of most cities, vegetation degraded, and productivity declined, indicating that urbanization has led to the loss of vegetation [62]. In addition, studies have shown that the interaction of temperature, precipitation, and solar radiation has different effects on vegetation greening [63–65], and sustained warming and decreased precipitation are key factors in limiting vegetation growth [66]. In the past 20 years, the overall climate has been dry and warm, with a significant upward trend in temperature (0.42 °C/10 year) but no significant change in precipitation in southwest China [36,48]. The occurrence of extreme weather events and natural disasters hinders the growth of vegetation, resulting in a decline in regional vegetation coverage [13,67]. In recent decades, severe droughts have occurred frequently in southwest China [68–71], which have had a significant impact on grassland and cropland. The average NDVI in the vegetation growing season has shown a decreasing trend (Figure 3b). However, the area of forest in this study region was about 2.4 times that of cropland, and the increase in the greening effect on the whole region compensated for the decreasing trend of NDVI.

The productivity levels of different LULC types had different responses to influencing factors. For example, cropland and grassland were vulnerable to extreme climate disasters, but the positive effects of human activities on the effective management of cropland weakened the negative effects of drought. From 2000 to 2019, the area of cropland decreased, but the average GPP value in the growing season showed an increasing trend in southwest China (p < 0.01), which may be related to the improvement in the productivity of cropland by agricultural management measures in recent years [24]. The forest ecosystem was relatively stable, and human activities, such as deforestation and afforestation, had a greater impact on the productivity of the forest ecosystem than the impact of extreme climates [72]. The average GPP of forest in the growing season showed a significant increasing trend, which was related to the increase in forest area and vegetation restoration in this region [73]. Studies have shown that vegetation productivity exhibits different growth patterns at different stages of forest age [74,75]. Due to the conversion of grassland to other land types, the amount of grassland has been decreasing continuously for 20 years. However, with the influence of ecosystem protection policies in recent years, the GPP of grassland still showed a fluctuating growth trend (Figure 4a). These results indicate that the overall carbon sequestration capacity of the southwest region is gradually increasing, and the environmental quality of the ecosystem is gradually improving, which corresponds to the significant increase in the vegetation coverage in southwest China in recent years.

Land 2022, 11, 1331 12 of 18

4.2. Migration Changes in NDVI and GPP Centroid

Our study indicated that the migration direction of the NDVI center of gravity of cropland, forest, and grassland was the same as that of GPP during 2000-2019 in southwest China (Figure 5), and the spatial distribution pattern of vegetation cover and productivity gravity center changed with a change in LULC distribution. In southwest China, the center of gravity of cropland moved westward, and there were inflection points of the center of gravity in 2001 and 2005. In 2001, the project of returning cropland to forest, ecological protection in the east, and the natural forest protection plan in the west were fully launched. Therefore, the area of cropland increased, and the area of forest decreased during 2000–2005. After 2005, ecological engineering began to achieve results, which showed that the cropland area decreased and the forest area increased, which was consistent with the results of previous studies [76]. These results indicated that the LULC change caused by the ecological restoration project was the direct cause of the change in the vegetation growth and productivity center of gravity in southwest China over the past 20 years. The inflection point times of the change in the center of gravity were consistent with the planning and implementation time of the restoration project. The grassland continued to migrate to the northwest, which may be related to the conversion of grassland to other land types in the southeast, while the northwest region had a higher altitude, less human activity, and fewer changes in land cover types [36]. The study also found that the change in GPP's gravity centers of different vegetation NDVI grades was highly similar to the migration direction of NDVI's gravity center changes of different grades (Figure A1). This indicated that the increase or decrease in vegetation productivity in southwest China was related to the restoration or degradation of vegetation; the productivity increased in the region of vegetation restoration, and the productivity decreased in the region of vegetation degradation. From 2000 to 2019, the change in the center of gravity of the lowest coverage was relatively stable, and the direction and distance of the center of gravity were not large. The center of gravity of low coverage and high coverage mainly shifted to the southeast, and the center of gravity of medium coverage and high coverage mainly shifted to the northwest. This was mainly because of the spatial distribution, composition, and climatic characteristics of LULC types of different vegetation grades at different stages, which affected the change in vegetation cover and the center of gravity of productivity. Therefore, reasonable planning of regional cover-type composition is of great significance to effectively improve regional vegetation NDVI and GPP.

The shift in vegetation types in the direction of the center of gravity indicates that the expansion of vegetation in the direction of migration or the degradation of vegetation in the opposite direction, and the long-term shift in the center of gravity in a single direction, lead to the imbalance of ecosystem structure and function. For example, the southern and southwestern regions of southwest China are the main regions of returning farmland to forest. Due to the favorable ecological conditions in this region, the vegetation coverage has shifted from medium coverage to high coverage. Recent studies have also confirmed that afforestation measures have achieved good results in improving vegetation cover and promoting carbon sequestration [58,77]. However, it was also found that the excessive growth of large regions of forest consumes surface water, resulting in a shortage of regional water resources [78,79]. In addition, local negative effects have also occurred due to the planting of unsuitable tree species [80]. To sum up, large-scale afforestation may rapidly improve the vegetation greening degree in the region in the short term, but it cannot guarantee the long-term stable development of the ecological environment. In addition, because of the heterogeneity of the growth of different vegetation types, it is understood that the composition structure of land cover types will affect the ecosystem balance and sustainable development in the southwest region of southwest China under different topographic and landform conditions.

4.3. Implications for Future

Our study found that the LULC change was beneficial to the improvement in regional greening and plant productivity in southwest China. Karst landforms are widely

Land 2022, 11, 1331 13 of 18

distributed in the study area. Due to its unique binary structure, precipitation is rapidly lost, which leads to low utilization of precipitation by vegetation [81]. Moreover, the karst regions have thin soil layers and poor water storage capacities, and the climate warming trend may have an inhibitory effect on the growth of forests [14]. Studies have shown that ecological restoration and LULC pattern change not only ameliorate land degradation [40] but also affect local and regional climate [82]. For example, land surface temperature decreases significantly when forest is converted to cropland [83]. The global warming trend has a greater impact on ecosystems [84,85], which has led to dramatic changes in land cover types and plant biomass in the high northern latitudes and promoted the expansion of woody shrubs and forest areas [86]. Meanwhile, the rise in temperature has removed local environmental boundaries, allowing alpine plant species to move to higher altitudes [87]. These results indicate that in future implementations of ecological projects, it is necessary to consider the structural composition and environmental carrying capacity of LULC types under the background of climate warming so that they can more effectively serve the maintenance of local, sustainable ecosystem balance.

5. Conclusions

We investigated NDVI and GPP in the growing season and changes in the spatiotemporal variation patterns of their centers of gravity in southwest China from 2000 to 2019. We found that the LULC structure of the study area changed greatly from 2000 to 2019. The area of forest increased while the area of cropland and grassland decreased, and cropland was the main contributor to the forest increase. For the entire study region, both NDVI and GPP in the growing season showed a generally increasing trend. However, there were differences in the increasing trend of NDVI and GPP among different LULC types. From the perspective of spatial distribution, NDVI and GPP showed a distribution pattern of high in the southeast and low in the northwest, corresponding to the fact that forest is mainly distributed in the southeast and grassland is concentrated in the northwest; the ecological restoration project has greatly improved the vegetation coverage, 45.6% of the region showed a greening trend. In 2000, it was dominated by medium coverage and high coverage (32.32%, 54.73%), while high coverage and highest coverage predominated in 2019 (49.29%, 34.37%). Under the same vegetation coverage, the spatiotemporal variation distribution of the center of gravity of NDVI and GPP was basically the same. From 2000 to 2019, the spatial variation in the center of gravity of NDVI and GPP at the lowest coverage was relatively stable; the center of gravity of low coverage shifted to the east, the center of gravity of medium coverage and the high coverage both shifted to the northwest, and the center of gravity of the highest coverage moved to the southeast. This indicates that although the southwest region is greening, there are differences in vegetation growth and carbon sequestration capacity among different land cover types, resulting in changes in the vegetation center of gravity. Therefore, the combination structure of vegetation cover and land cover type should be prioritized in the future to ensure the balance of the ecosystem in the southwest and maintain sustainable development.

Author Contributions: Conceptualization, L.R. and X.L.; methodology, X.L.; software, M.Z. and C.Y.; formal analysis, X.L. and W.Y.; investigation, M.Z., Q.W., Z.Z., and C.Y.; data curation, X.L.; writing—original draft preparation, X.L.; writing—review and editing, L.R. and X.L.; visualization, X.L.; supervision, X.L.; project administration, X.L.; funding acquisition, L.R. All authors have read and agreed to the published version of the manuscript.

Funding: This research was funded by the key project of the "14th Five-Year" National Key R&D Program "Typical Fragile Ecosystem Protection and Restoration", grant number "2022YFC080900" and the Karst plateau canyon rocky desertification comprehensive control and scale management technology and demonstration of ecological industry, grant number "2016YFC0502603", Project of National "Thirteenth Five-year" Key Research and Development Programme.

Institutional Review Board Statement: Not applicable.

Informed Consent Statement: Informed consent was obtained from all subjects involved in the study.

Land 2022, 11, 1331 14 of 18

Data Availability Statement: Not applicable.

Acknowledgments: We thank the anonymous reviewers for their valuable comments. We gratefully acknowledge the design of L.R. and the contribution of co-authors.

Conflicts of Interest: The authors declare no conflict of interest.

Appendix A

Table A1. Transformation matrix of NDVI grades from 2000 to 2019 (km²).

2000–2019	0~0.35	0.35~0.55	0.55~0.75	0.75~0.85	0.85~1.0
0~0.35	4397.62	2772.06	630.53	95.78	45.96
0.35~0.55	1089.16	11,384.48	11,465.65	1269.25	169.92
$0.55 \sim 0.75$	418.50	8424.23	136,924.63	259,673.48	39,192.96
$0.75 \sim 0.85$	57.80	1560.78	44,215.18	395,140.43	311,870.61
0.85~1.0	5.03	48.18	1050.40	22,088.73	121,421.98

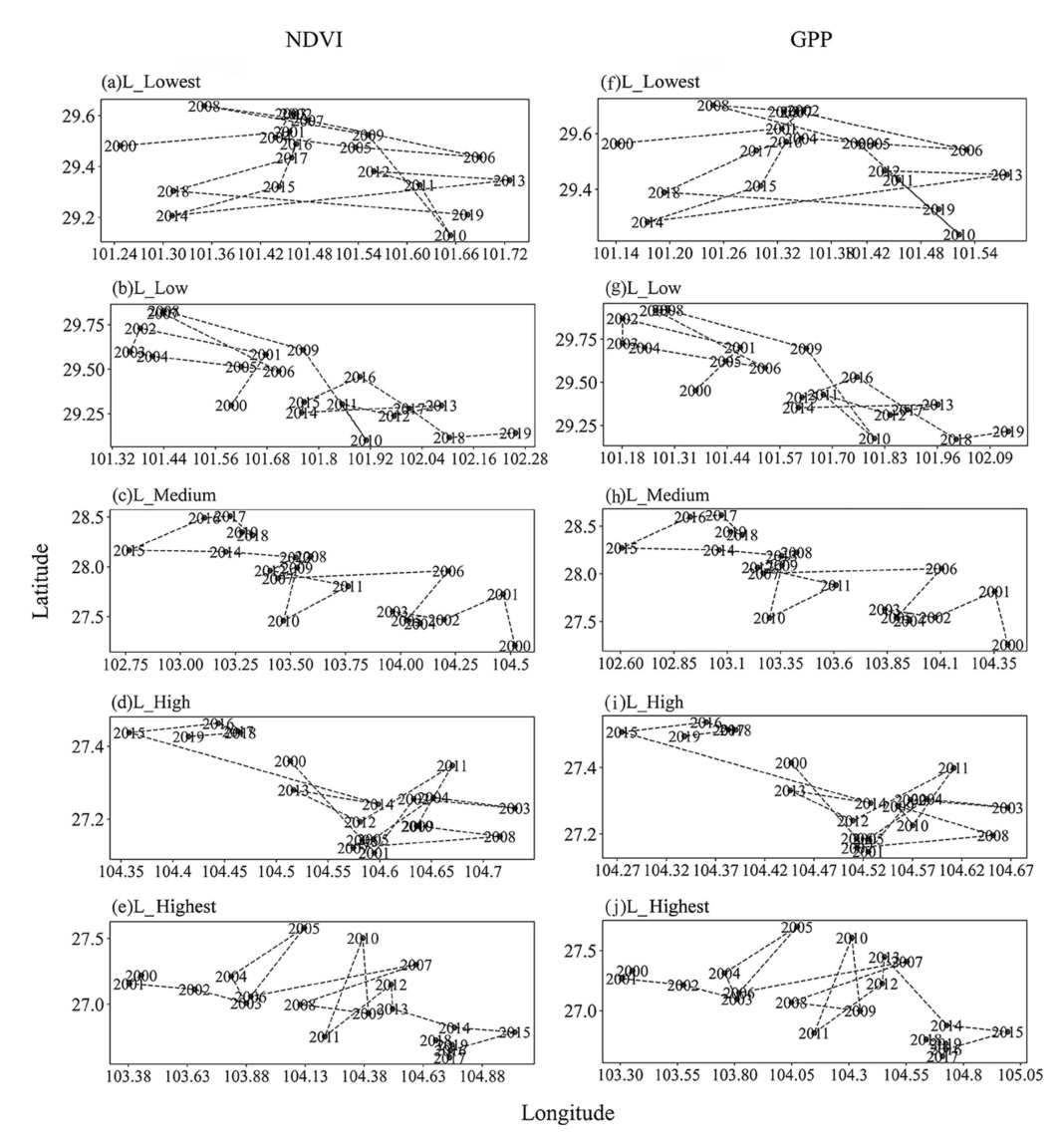


Figure A1. Variation in the center of gravity of different NDVI grades and its GPP. (Note: (a-e): Changes in the center of gravity of the five NDVI grades from 2000 to 2019; (f-j): Changes in the center of gravity of GPP for five NDVI grades from 2000 to 2019).

Land 2022, 11, 1331 15 of 18

References

1. Liu, H.; Zhang, M.; Lin, Z.; Xu, X. Spatial heterogeneity of the relationship between vegetation dynamics and climate change and their driving forces at multiple time scales in Southwest China. *Agric. For. Meteorol.* **2018**, 256, 10–21. [CrossRef]

- 2. Yan, W.; Wang, H.; Jiang, C.; Jin, S.; Ai, J.; Sun, O.J. Satellite view of vegetation dynamics and drivers over southwestern China. *Ecol. Indic.* **2021**, *130*, 108074. [CrossRef]
- 3. Huang, J.; Ge, Z.; Huang, Y.; Tang, X.; Shi, Z.; Lai, P.; Song, Z.; Hao, B.; Yang, H.; Ma, M. Climate change and ecological engineering jointly induced vegetation greening in global karst regions from 2001 to 2020. *Plant Soil* **2022**, *475*, 193–212. [CrossRef]
- 4. Yue, Y.; Liao, C.; Tong, X.; Wu, Z.; Fensholt, R.; Prishchepov, A.; Jepsen, M.R.; Wang, K.; Brandt, M. Large scale reforestation of farmlands on sloping hills in South China karst. *Landsc. Ecol.* **2020**, *35*, 1445–1458. [CrossRef]
- 5. Li, Y.; Zhang, Y.; Lv, J. Interannual variations in GPP in forest ecosystems in Southwest China and regional differences in the climatic contributions. *Ecol. Inform.* **2022**, *69*, 101591. [CrossRef]
- Luo, X.; Jia, B.; Lai, X. Contributions of climate change, land use change and CO₂ to changes in the gross primary productivity of the Tibetan Plateau. Atmos. Ocean. Sci. Lett. 2020, 13, 8–15. [CrossRef]
- 7. Tian, S.; Wang, S.; Bai, X.; Luo, G.; Li, Q.; Yang, Y.; Hu, Z.; Li, C.; Deng, Y. Global patterns and changes of carbon emissions from land use during 1992–2015. *Environ. Sci. Ecotechnol.* **2021**, 7, 100108. [CrossRef]
- 8. Zhu, L.; Song, R.; Sun, S.; Li, Y.; Hu, K. Land use/land cover change and its impact on ecosystem carbon storage in coastal areas of China from 1980 to 2050. *Ecol. Indic.* **2022**, *142*, 109178. [CrossRef]
- 9. Fang, Z.; Ding, T.; Chen, J.; Xue, S.; Zhou, Q.; Wang, Y.; Wang, Y.; Huang, Z.; Yang, S. Impacts of land use/land cover changes on ecosystem services in ecologically fragile regions. *Sci. Total Environ.* **2022**, *831*, 154967. [CrossRef]
- Jiang, Z.; Lian, Y.; Qin, X. Rocky desertification in Southwest China: Impacts, causes, and restoration. Earth Sci. Rev. 2014, 132, 1–12. [CrossRef]
- 11. Dai, Q.; Peng, X.; Yang, Z.; Zhao, L. Runoff and erosion processes on bare slopes in the karst rocky desertification area. *CATENA* **2017**, *152*, 218–226. [CrossRef]
- 12. Mokhtar, A.; He, H.; Alsafadi, K.; Li, Y.; Zhao, H.; Keo, S.; Bai, C.; Abuarab, M.; Zhang, C.; Elbagoury, K.; et al. Evapotranspiration as a response to climate variability and ecosystem changes in southwest, China. *Environ. Earth Sci.* **2020**, *79*, 312. [CrossRef]
- 13. Ali, S.; Haixing, Z.; Qi, M.; Liang, S.; Ning, J.; Jia, Q.; Hou, F. Monitoring drought events and vegetation dynamics in relation to climate change over mainland China from 1983 to 2016. *Environ. Sci. Pollut. Res.* **2021**, *28*, 21910–21925. [CrossRef] [PubMed]
- 14. Sun, H.; Wang, X.; Fan, D.; Sun, O.J. Contrasting vegetation response to climate change between two monsoon regions in Southwest China: The roles of climate condition and vegetation height. *Sci. Total Environ.* **2022**, *802*, 149643. [CrossRef] [PubMed]
- 15. Bai, X.Y.; Wang, S.-J.; Xiong, K.-N. Assessing spatial-temporal evolution processes of karst rocky desertification land: Indications for restoration strategies. *Land Degrad. Dev.* **2013**, 24, 47–56. [CrossRef]
- 16. Sweeting, M.M. Karst in China: Its Geomorphology and Environment; Springer: Berlin/Heidelberg, Germany, 2012; Volume 15.
- 17. Zhu, Z.; Piao, S.; Myneni, R.B.; Huang, M.; Zeng, Z.; Canadell, J.G.; Ciais, P.; Sitch, S.; Friedlingstein, P.; Arneth, A.; et al. Greening of the Earth and its drivers. *Nat. Clim. Chang.* **2016**, *6*, 791–795. [CrossRef]
- 18. Zheng, K.; Wei, J.-Z.; Pei, J.-Y.; Cheng, H.; Zhang, X.-L.; Huang, F.-Q.; Li, F.-M.; Ye, J.-S. Impacts of climate change and human activities on grassland vegetation variation in the Chinese Loess Plateau. *Sci. Total Environ.* **2019**, *660*, 236–244. [CrossRef]
- 19. Liu, J.; Kuang, W.; Zhang, Z.; Xu, X.; Qin, Y.; Ning, J.; Zhou, W.; Zhang, S.; Li, R.; Yan, C.; et al. Spatiotemporal characteristics, patterns, and causes of land-use changes in China since the late 1980s. *J. Geogr. Sci.* **2014**, 24, 195–210. [CrossRef]
- 20. Fang, J.; Guo, Z.; Hu, H.; Kato, T.; Muraoka, H.; Son, Y. Forest biomass carbon sinks in E ast A sia, with special reference to the relative contributions of forest expansion and forest growth. *Glob. Chang. Biol.* **2014**, *20*, 2019–2030. [CrossRef]
- 21. Ouyang, Z.; Zheng, H.; Xiao, Y.; Polasky, S.; Liu, J.; Xu, W.; Wang, Q.; Zhang, L.; Xiao, Y.; Rao, E.; et al. Improvements in ecosystem services from investments in natural capital. *Science* **2016**, 352, 1455–1459. [CrossRef]
- 22. Li, C.; Bai, X.; Tan, Q.; Luo, G.; Wu, L.; Chen, F.; Xi, H.; Luo, X.; Ran, C.; Chen, H.; et al. High-resolution mapping of the global silicate weathering carbon sink and its long-term changes. *Glob. Chang. Biol.* **2022**, 28, 4377–4394. [CrossRef] [PubMed]
- 23. Tian, Y.; Wang, S.; Bai, X.; Luo, G.; Xu, Y. Trade-offs among ecosystem services in a typical Karst watershed, SW China. *Sci. Total Environ.* **2016**, 566, 1297–1308. [CrossRef] [PubMed]
- 24. Chen, C.; Park, T.; Wang, X.; Piao, S.; Xu, B.; Chaturvedi, R.K.; Fuchs, R.; Brovkin, V.; Ciais, P.; Fensholt, R.; et al. China and India lead in greening of the world through land-use management. *Nat. Sustain.* **2019**, 2, 122–129. [CrossRef] [PubMed]
- 25. Xiong, L.; Bai, X.; Zhao, C.; Li, Y.; Tan, Q.; Luo, G.; Wu, L.; Chen, F.; Li, C.; Ran, C.; et al. High-resolution datasets for global carbonate and silicate rock weathering carbon sinks and their change trends. *Earth's Future* **2022**, *10*, e2022EF002746. [CrossRef]
- 26. Brandt, M.; Yue, Y.; Wigneron, J.-P.; Tong, X.; Tian, F.; Jepsen, M.R.; Xiao, X.; Verger, A.; Mialon, A.; Al-Yaari, A.; et al. Satellite-observed major greening and biomass increase in south China karst during recent decade. *Earths Future* **2018**, *6*, 1017–1028. [CrossRef]
- 27. Zhang, S.; Bai, X.; Zhao, C.; Tan, Q.; Luo, G.; Wu, L.; Xi, H.; Li, C.; Chen, F.; Ran, C.; et al. China's carbon budget inventory from 1997 to 2017 and its challenges to achieving carbon neutral strategies. *J. Clean. Prod.* **2022**, 347, 130966. [CrossRef]
- 28. Pettorelli, N.; Vik, J.O.; Mysterud, A.; Gaillard, J.-M.; Tucker, C.J.; Stenseth, N.C. Using the satellite-derived NDVI to assess ecological responses to environmental change. *Trends Ecol. Evol.* **2005**, *20*, 503–510. [CrossRef]
- 29. Fensholt, R.; Proud, S.R. Evaluation of earth observation based global long term vegetation trends—Comparing GIMMS and MODIS global NDVI time series. *Remote Sens. Environ.* **2012**, *119*, 131–147. [CrossRef]

Land 2022, 11, 1331 16 of 18

30. Zhang, X.; Liu, K.; Li, X.; Wang, S.; Wang, J. Vulnerability assessment and its driving forces in terms of NDVI and GPP over the Loess Plateau, China. *Phys. Chem. Earth, Parts A/B/C* **2022**, *125*, 103106. [CrossRef]

- 31. Wang, Z.; Liu, S.; Wang, Y.; Valbuena, R.; Wu, Y.; Kutia, M.; Zheng, Y.; Lu, W.; Zhu, Y.; Zhao, M.; et al. Tighten the Bolts and Nuts on GPP Estimations from Sites to the Globe: An Assessment of Remote Sensing Based LUE Models and Supporting Data Fields. *Remote Sens.* **2021**, *13*, 168. [CrossRef]
- 32. Ito, A.; Inatomi, M.; Huntzinger, D.N.; Schwalm, C.; Michalak, A.M.; Cook, R.; King, A.W.; Mao, J.; Wei, Y.; Mac Post, W.; et al. Decadal trends in the seasonal-cycle amplitude of terrestrial CO₂ exchange resulting from the ensemble of terrestrial biosphere models. *Tellus B Chem. Phys. Meteorol.* **2016**, *68*, 28968. [CrossRef]
- 33. Piao, S.; Sitch, S.; Ciais, P.; Friedlingstein, P.; Peylin, P.; Wang, X.; Ahlström, A.; Anav, A.; Canadell, J.G.; Cong, N.; et al. Evaluation of terrestrial carbon cycle models for their response to climate variability and to CO₂ trends. *Glob. Chang. Biol.* **2013**, *19*, 2117–2132. [CrossRef] [PubMed]
- 34. Wu, L.; Wang, S.; Bai, X.; Tian, Y.; Luo, G.; Wang, J.; Li, Q.; Chen, F.; Deng, Y.; Yang, Y.; et al. Climate change weakens the positive effect of human activities on karst vegetation productivity restoration in southern China. *Ecol. Indic.* **2020**, *115*, 106392. [CrossRef]
- 35. Chen, Y.; Wang, S.; Wang, Y. Spatiotemporal Evolution of Cultivated Land Non-Agriculturalization and Its Drivers in Typical Areas of Southwest China from 2000 to 2020. *Remote Sens.* **2022**, *14*, 3211. [CrossRef]
- 36. Jiang, S.; Chen, X.; Smettem, K.; Wang, T. Climate and land use influences on changing spatiotemporal patterns of mountain vegetation cover in southwest China. *Ecol. Indic.* **2021**, *121*, 107193. [CrossRef]
- 37. Ding, Z.; Zheng, H.; Liu, Y.; Zeng, S.; Yu, P.; Shi, W.; Tang, X. Spatiotemporal Patterns of Ecosystem Restoration Activities and Their Effects on Changes in Terrestrial Gross Primary Production in Southwest China. *Remote Sens.* **2021**, *13*, 1209. [CrossRef]
- 38. Tan, Z.; Tao, H.; Jiang, J.; Zhang, Q. Influences of climate extremes on NDVI (normalized difference vegetation index) in the Poyang Lake Basin, China. *Wetlands* **2015**, *35*, 1033–1042. [CrossRef]
- 39. Wang, W.; Wang, W.J.; Li, J.S.; Wu, H.; Xu, C.; Liu, T. The impact of sustained drought on vegetation ecosystem in Southwest China based on remote sensing. *Procedia Environ. Sci.* **2010**, *2*, 1679–1691. [CrossRef]
- 40. Tong, X.; Brandt, M.; Yue, Y.; Horion, S.; Wang, K.; De Keersmaecker, W.; Tian, F.; Schurgers, G.; Xiao, X.; Luo, Y.; et al. Increased vegetation growth and carbon stock in China karst via ecological engineering. *Nat. Sustain.* **2018**, *1*, 44–50. [CrossRef]
- 41. Yue, X.; Zhang, T.; Shao, C. Afforestation increases ecosystem productivity and carbon storage in China during the 2000s. *Agric. For. Meteorol.* **2021**, 296, 108227. [CrossRef]
- 42. Xiao, J.; Zhou, Y.; Zhang, L. Contributions of natural and human factors to increases in vegetation productivity in China. *Ecosphere* **2015**, *6*, art233–20. [CrossRef]
- 43. Hurtt, G.C.; Chini, L.P.; Frolking, S.; Betts, R.A.; Feddema, J.; Fischer, G.; Fisk, J.P.; Hibbard, K.; Houghton, R.A.; Janetos, A.; et al. Harmonization of land-use scenarios for the period 1500–2100: 600 years of global gridded annual land-use transitions, wood harvest, and resulting secondary lands. *Clim. Chang.* **2011**, *109*, 117–161. [CrossRef]
- 44. Zhao, A.; Zhang, A.; Liu, X.; Cao, S. Spatiotemporal changes of normalized difference vegetation index (NDVI) and response to climate extremes and ecological restoration in the Loess Plateau, China. *Arch. Meteorol. Geophys. Bioclimatol. Ser. B* **2018**, 132, 555–567. [CrossRef]
- 45. Piao, S.; Fang, J.; Ji, W.; Guo, Q.; Ke, J.; Tao, S. Variation in a satellite-based vegetation index in relation to climate in China. *J. Veg. Sci.* 2004, 15, 219–226. [CrossRef]
- 46. Liu, H.; Gong, P.; Wang, J.; Clinton, N.; Bai, Y.; Liang, S. Annual dynamics of global land cover and its long-term changes from 1982 to 2015. *Earth Syst. Sci. Data* **2020**, *12*, 1217–1243. [CrossRef]
- 47. Rundqvist, S.; Hedenås, H.; Sandström, A.; Emanuelsson, U.; Eriksson, H.; Jonasson, C.; Callaghan, T.V. Tree and shrub expansion over the past 34 years at the tree-line near Abisko, Sweden. *Ambio* **2011**, *40*, 683–692. [CrossRef]
- 48. Lian, Y.; You, G.J.-Y.; Lin, K.; Jiang, Z.; Zhang, C.; Qin, X. Characteristics of climate change in southwest China karst region and their potential environmental impacts. *Environ. Earth Sci.* **2015**, *74*, 937–944. [CrossRef]
- 49. Yang, J.; Huang, X. 30 m annual land cover and its dynamics in China from 1990 to 2019. Earth Syst. Sci. Data Discuss. 2021, 1–29.
- 50. Piao, S.; Fang, J.; Zhou, L.; Guo, Q.; Henderson, M.; Ji, W.; Li, Y.; Tao, S. Interannual variations of monthly and seasonal normalized difference vegetation index (NDVI) in China from 1982 to 1999. *J. Geophys. Res. Earth Surf.* 2003, 108, 4401. [CrossRef]
- 51. Zhang, Y.; Zhu, Z.; Liu, Z.; Zeng, Z.; Ciais, P.; Huang, M.; Liu, Y.; Piao, S. Seasonal and interannual changes in vegetation activity of tropical forests in Southeast Asia. *Agric. For. Meteorol.* **2016**, 224, 1–10. [CrossRef]
- 52. Hou, W.; Gao, J.; Wu, S.; Dai, E. Interannual variations in growing-season NDVI and its correlation with climate variables in the southwestern karst region of China. *Remote Sens.* **2015**, *7*, 11105–11124. [CrossRef]
- 53. Holben, B.N. Characteristics of maximum-value composite images from temporal AVHRR data. *Int. J. Remote Sens.* **1986**, 7, 1417–1434. [CrossRef]
- 54. Yuan, L.; Chen, X.; Wang, X.; Xiong, Z.; Song, C. Spatial associations between NDVI and environmental factors in the Heihe River Basin. *J. Geogr. Sci.* **2019**, 29, 1548–1564. [CrossRef]
- 55. Pei, J.; Wang, L.; Wang, X.; Niu, Z.; Kelly, M.; Song, X.-P.; Huang, N.; Geng, J.; Tian, H.; Yu, Y.; et al. Time series of Landsat imagery shows vegetation recovery in two fragile karst watersheds in southwest china from 1988 to 2016. *Remote Sens.* **2019**, *11*, 2044. [CrossRef]
- 56. López, E.; Bocco, G.; Mendoza, M.; Duhau, E. Predicting land-cover and land-use change in the urban fringe: A case in Morelia city, Mexico. *Landsc. Urban Plan.* **2001**, *55*, 271–285. [CrossRef]

Land 2022, 11, 1331 17 of 18

57. Liu, J.; Zhang, Z.; Xu, X.; Kuang, W.; Zhou, W.; Zhang, S.; Li, R.; Yan, C.; Yu, D.; Wu, S.; et al. Spatial patterns and driving forces of land use change in China during the early 21st century. *J. Geogr. Sci.* **2010**, 20, 483–494. [CrossRef]

- 58. Lu, F.; Hu, H.; Sun, W.; Zhu, J.; Liu, G.; Zhou, W.; Zhang, Q.; Shi, P.; Liu, X.; Wu, X.; et al. Effects of national ecological restoration projects on carbon sequestration in China from 2001 to 2010. *Proc. Natl. Acad. Sci. USA* 2018, 115, 4039–4044. [CrossRef]
- 59. Chen, Y.; Chen, L.; Cheng, Y.; Ju, W.; Chen, H.Y.H.; Ruan, H. Afforestation promotes the enhancement of forest LAI and NPP in China. For. Ecol. Manag. 2020, 462, 117990. [CrossRef]
- 60. Zhang, S.; Bai, X.; Zhao, C.; Tan, Q.; Luo, G.; Cao, Y.; Deng, Y.; Li, Q.; Li, C.; Wu, L.; et al. Limitations of soil moisture and formation rate on vegetation growth in karst areas. *Sci. Total Environ.* **2022**, *810*, 151209. [CrossRef]
- 61. Pan, Y.; Birdsey, R.A.; Fang, J.; Houghton, R.; Kauppi, P.E.; Kurz, W.A.; Phillips, O.L.; Shvidenko, A.; Lewis, S.L.; Canadell, J.G.; et al. A large and persistent carbon sink in the world's forests. *Science* **2011**, *333*, 988–993. [CrossRef]
- 62. Deng, J.S.; Wang, K.; Hong, Y.; Qi, J.G. Spatio-temporal dynamics and evolution of land use change and landscape pattern in response to rapid urbanization. *Landsc. Urban Plan.* **2009**, 92, 187–198. [CrossRef]
- 63. Nemani, R.R.; Keeling, C.D.; Hashimoto, H.; Jolly, W.M.; Piper, S.C.; Tucker, C.J.; Myneni, R.B.; Running, S.W. Climate-driven increases in global terrestrial net primary production from 1982 to 1999. *Science* 2003, 300, 1560–1563. [CrossRef] [PubMed]
- 64. Forzieri, G.; Alkama, R.; Miralles, D.G.; Cescatti, A. Satellites reveal contrasting responses of regional climate to the widespread greening of Earth. *Science* **2017**, *356*, 1180–1184. [CrossRef] [PubMed]
- 65. Yang, H.; Hu, J.; Zhang, S.; Xiong, L.; Xu, Y. Climate Variations vs. Human Activities: Distinguishing the Relative Roles on Vegetation Dynamics in the Three Karst Provinces of Southwest China. *Front. Earth Sci.* **2022**, *10*, 799493. [CrossRef]
- 66. Piao, S.; Wang, X.; Ciais, P.; Zhu, B.; Wang, T.; Liu, J. Changes in satellite-derived vegetation growth trend in temperate and boreal Eurasia from 1982 to 2006. *Glob. Chang. Biol.* **2011**, *17*, 3228–3239. [CrossRef]
- 67. Guan, Y.; Zheng, F.; Zhang, P.; Qin, C. Spatial and temporal changes of meteorological disasters in China during 1950–2013. *Nat. Hazards* **2015**, *75*, 2607–2623. [CrossRef]
- 68. Peng, J.; Zhang, Q.Y.; Bueh, C. On the characteristics and possible causes of a severe drought and heat wave in the Sichuan-Chongqing region in 2006. *Clim. Environ. Res.* **2007**, 12, 464–474.
- 69. Huang, R.; Liu, Y.; Wang, L.; Wang, L. Analyses of the causes of severe drought occurring in Southwest China from the fall of 2009 to the spring of 2010. *Chin. J. Atmos. Sci.* 2012, *36*, 443–457.
- 70. Sun, L.; Ren, F.M.; Wang, Z.Y.; Liu, Y.Y.; Liu, Y.J.; Wang, P.L.; Wang, D.Q. Analysis of climate anomaly and causation in August 2011. *Meteorol. Mon.* 2012, 38, 615–622.
- 71. Huang, Y.; Xu, C.; Yang, H.; Wang, J.; Jiang, D.; Zhao, C. Temporal and spatial variability of droughts in southwest china from 1961 to 2012. *Sustainability* **2015**, *7*, 13597–13609. [CrossRef]
- 72. Qiao, Y.; Jiang, Y.; Zhang, C. Contribution of karst ecological restoration engineering to vegetation greening in southwest China during recent decade. *Ecol. Indic.* **2021**, *121*, 107081. [CrossRef]
- 73. Tong, X.; Brandt, M.; Yue, Y.; Ciais, P.; Rudbeck Jepsen, M.; Penuelas, J.; Wigneron, J.-P.; Xiao, X.-P.; Song, X.-P.; Horion, S.; et al. Forest management in southern China generates short term extensive carbon sequestration. *Nat. Commun.* **2020**, *11*, 129. [CrossRef] [PubMed]
- 74. Wang, S.; Zhou, L.; Chen, J.; Ju, W.; Feng, X.; Wu, W. Relationships between net primary productivity and stand age for several forest types and their influence on China's carbon balance. *J. Environ. Manag.* **2011**, 92, 1651–1662. [CrossRef] [PubMed]
- 75. He, L.; Chen, J.M.; Pan, Y.; Birdsey, R.A.; Kattge, J. Relationships between net primary productivity and forest stand age in US forests. *Glob. Biogeochem. Cycles* **2012**, *26*, 394–415. [CrossRef]
- 76. Xu, X.; Liu, H.; Lin, Z.; Jiao, F.; Gong, H. Relationship of abrupt vegetation change to climate change and ecological engineering with multi-timescale analysis in the karst region, Southwest China. *Remote Sens.* **2019**, *11*, 1564. [CrossRef]
- 77. Zhang, C. Carbonate rock dissolution rates in different landuses and their carbon sink effect. *Chin. Sci. Bull.* **2011**, *56*, 3759–3765. [CrossRef]
- 78. Škerlep, M.; Steiner, E.; Axelsson, A.L.; Kritzberg, E.S. Afforestation driving long-term surface water browning. *Glob. Chang. Biol.* **2020**, *26*, 1390–1399. [CrossRef]
- 79. Feng, X.; Fu, B.; Piao, S.; Wang, S.; Ciais, P.; Zeng, Z.; Lü, Y.; Zeng, Y.; Li, Y.; Jiang, X.; et al. Revegetation in China's Loess Plateau is approaching sustainable water resource limits. *Nat. Clim. Chang.* **2016**, *6*, 1019–1022. [CrossRef]
- 80. Zhang, L.; Sun, P.; Huettmann, F.; Liu, S. Where should China practice forestry in a warming world? *Glob. Chang. Biol.* **2022**, *28*, 2461–2475. [CrossRef]
- 81. Zhou, Q.; Luo, Y.; Zhou, X.; Cai, M.; Zhao, C. Response of vegetation to water balance conditions at different time scales across the karst area of southwestern China—A remote sensing approach. *Sci. Total Environ.* **2018**, 645, 460–470. [CrossRef]
- 82. Peng, S.-S.; Piao, S.; Zeng, Z.; Ciais, P.; Zhou, L.; Li, L.Z.X.; Myneni, R.B.; Yin, Y.; Zeng, H. Afforestation in China cools local land surface temperature. *Proc. Natl. Acad. Sci. USA* **2014**, *111*, 2915–2919. [CrossRef] [PubMed]
- 83. Jiang, L.; Zhang, H.; Zhao, F.; Zhang, L.; Wang, X. Warming/cooling effect of cropland expansion during the 1900s~ 2010s in the Heilongjiang Province, Northeast of China. *Int. J. Biometeorol.* **2022**, *66*, 1379–1390. [CrossRef]
- 84. Heyder, U.; Schaphoff, S.; Gerten, D.; Lucht, W. Risk of severe climate change impact on the terrestrial biosphere. *Environ. Res. Lett.* **2011**, *6*, 034036. [CrossRef]
- 85. Xi, H.; Wang, S.; Bai, X.; Tang, H.; Luo, G.; Li, H.; Wu, L.; Li, C.; Chen, H.; Ran, C.; et al. The responses of weathering carbon sink to eco-hydrological processes in global rocks. *Sci. Total Environ.* **2021**, 788, 147706. [CrossRef] [PubMed]

Land **2022**, 11, 1331

86. Xue, S.-Y.; Xu, H.-Y.; Mu, C.-C.; Wu, T.-H.; Li, W.-P.; Zhang, W.-X.; Streletskaya, I.; Grebenets, V.; Sokratov, S.; Kizyakov, A.; et al. Changes in different land cover areas and NDVI values in northern latitudes from 1982 to 2015. *Adv. Clim. Chang. Res.* **2021**, 12, 456–465. [CrossRef]

87. Vanneste, T.J.M. Climate Change and Alpine Vegetation Shifts on Mountaintop Summits in Norway. Ph.D. Thesis, Universiteit Gent, Gent, Belgium, 2016.